SPIDERMAN SPACECRAFT: TETHERED ASTEROID HOPPING IN THE MAIN BELT

Alexander Wittig, Dario Izzo

ESA Advanced Concepts Team, ESTEC, 2200AG Noordwijk, The Netherlands
{alexander.wittig, dario.izzo}@esa.int

ABSTRACT

The use of the gravity of celestial bodies for gravity assist maneuvers is quite common in astrodynamics. The spacecraft gravitationally interacts with the celestial body in such a way as to provide the desired delta-v to the spacecraft. While this works well for large bodies such as planets, the gravitational attraction of small bodies, such as asteroids, is typically too small to perform such maneuvers.

In this paper we analyze a different type of fly-by orbit using a variable length tether. During a fly-by of the spacecraft at an asteroid, a tether is attached to the asteroid which is then reeled out maintaining a constant tension within the limits of the tether. A dynamical model describing such a tethered flyby is developed. Using this model, it is possible to perform fly-by maneuvers that conceptually are very similar to traditional gravity assist maneuvers. Unlike various previously reported tethered trajectory designs, these flybys are within the realm of feasibility already with currently existing tether technology.

We demonstrate a potential use of such tethered flyby maneuvers for the design of multiple asteroid rendezvous orbits. A spacecraft in the main asteroid belt has to visit a sequence of asteroids via tethered flybys. The required change in velocity is achieved mainly through the tethered flyby aided by one chemical burn. Optimization is performed with respect to the required Δv provided by chemical propulsion. The computation is performed using the PyKEP and PyGMO toolboxes developed by the Advanced Concepts Team. Due to its flexible open source design, this Python based toolbox can easily be modified to include these novel fly-by dynamics.

Index Terms— flyby, asteroid, tether, sequence, gravity assist

1. INTRODUCTION

Since the 1960 classical gravity assist maneuvers around planets and their moons have been a standard tool in the design of interplanetary trajectories [1]. Due to their low gravitational field, asteroids are not suitable for such maneuvers. However, using a tether to temporarily connect a spacecraft with an asteroid allows for tethered flyby maneuvers yielding a similar result. This mechanism was already proposed in of the earliest papers on the topic [2]. This work mostly focused on possible applications and the limits they place on the tether strength. subsequently, various models for the dynamics of tethered spacecraft motion have been developed over time, considering variations such as fixed and variable length tethers, fixed and varying cross-section tethers as well as different possible applications of tethered motion.

In [3] the complete dynamics of tethered motion including rotation of the asteroid, possible thrusting by the spacecraft during flyby, and variable tether cross-section profiles are developed. The resulting equations of motion are simplified and yield differential equations for the motion of the spacecraft. The authors then apply their dynamics to a near Earth asteroid mission. In [4], instead, the same simple tether dynamics of the original work by Penzo et al. is used to study the possibility of tethering two asteroids in order to effect a change in velocity of one of them in order to capture the asteroid for space mining. In [5] the authors study the same simple tether dynamics but in the setting of the circular restricted three body problem (CR3BP). The goal there is to use a tethered flyby of a moon to achieve subsequent capture of the spacecraft by the planet.

In this work, we study the possibility of a sequence of tethered flyby maneuvers of asteroids in the main asteroid belt using a variable length constant force tether. The spacecraft attaches a tether to various asteroids in order to obtain the required change in orbit to reach another asteroid, similar to the way the Spiderman comic character swings through the streets of New York by attaching spider silk to sky scrapers. While such an asteroid belt mission was already mentioned as a possibility in [2], to the best knowledge of the authors using tethered flybys to achieve such a sequence of flyby maneuvers in the main asteroid belt has never been implemented. Furthermore, due to the often simplified modeling the flyby dynamics the tension in the tethers are often unrealistically high [4, 5], leading to mechanically unfeasible requirements on the tether and the spacecraft structure. To avoid this, we develop the dynamics for a tension limited tether which ensures that the tension in the tether never exceeds a given maximum value. The tension required in the tether in our examples is achievable with currently commercially available tether materials. The resulting dynamics are solved analytically, yielding an explicit expression for the final deflection angle during
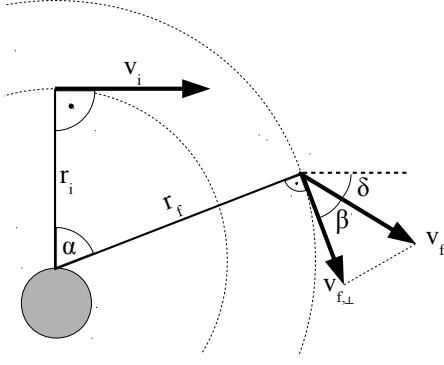
Fig. 1. Coordinate system of a tethered flyby.

the flyby in terms of an elliptic integral as a function of the parameters of the flyby. This allows the implementation of a flyby in a way very similar to classical gravity assist maneuvers in terms of a single parameter, the minimum flyby radius, yielding the final velocity after the flyby.

We begin by developing the equations governing a single flyby maneuver in Section 2 and continue to analyze their behavior in Section 3. This is followed by a discussion of the global search algorithm for a sequence of asteroid flybys in the main asteroid belt and its implementation within the PyKEP and PyGMO frameworks in Section 4. Finally we present some concluding remarks in Section 5.

2. FLYBY DYNAMICS

The flyby is modeled as starting at the closest approach of the spacecraft and the asteroid. We only consider the spacecraft dynamics after the tether is securely attached to the asteroid surface, neglecting the process of rolling out the tether and attaching it to the asteroid surface.

The coordinate system for the flyby is centered at the point on the asteroid surface where the tether is attached to the asteroid and the asteroid is assumed to be at rest. Since tethered flybys are generally quite fast, this is a reasonable assumption as both the non-inertial motion of the asteroid's center of mass due to the solar gravity as well as a possible rotation of the asteroid itself are several orders of magnitude slower than the flyby.

2.1. Dynamics

The initial distance from the surface of the asteroid to the spacecraft is given by r_i, while the initial velocity v_i is entirely in the tangential direction (see Figure 1). This means that the flyby begins at the distance of closest approach between asteroid and spacecraft.

The radial force exerted by the tether on the spacecraft is

modeled as

$$F_r = \begin{cases} -F & \dot{r} > 0 \\ \min(-F, -\frac{mv^2}{r}) & \dot{r} = 0 \\ 0 & \dot{r} < 0 \end{cases} \quad (1)$$

where F is the maximum force exerted on the spacecraft. This is a typical force law for a constant friction force. The force always acts against the outward motion but never adds energy to the spacecraft. Practically, this represents a tether being released while a friction force is being applied either to the tether directly or to the mechanism releasing the tether. The effect of this purely radial force is to reduce the radial velocity of the spacecraft as it passes by.

The initial angular momentum of the spacecraft is

$$L = mvr.$$

As this is a purely radial force, the angular momentum L is conserved. The force is obviously not conservative in the general case. However, while the spacecraft is only moving outwards ($\dot{r} > 0$) it can be represented by a potential of the form

$$P(r) = Fr. \quad (2)$$

From Equation 1 we can deduce that whenever $\dot{r} = 0$ there are two possible cases for the further dynamics: either $mv_i^2/r_i > F$, in which case the radial force F_r is less than the centripetal force required to maintain a circular orbit and hence $\ddot{r} > 0$. Otherwise, the radial force F_r is exactly equal to the centripetal force, thus maintaining a circular orbit and hence $\dot{r} = 0$ for all future times. Since the $\dot{r}$ is continuous, this implies that if $\dot{r} \geqslant 0$ at some time t_0, $\dot{r} \geqslant 0$ for all future times $t > t_0$. This justifies why we can consider this motion to be taking place in a potential of the form given in Equation 2 even if the radial force is not conservative.

The energy is then also conserved and given by

$$E = \frac{1}{2}mv^2 + Fr.$$

For our flybys we are interested only in orbits that are not permanently captured in a circular orbit, but that reach the final radius r_f given by the tether length when the tether is severed and the flyby ends. The two conditions for circular capture are $v_\perp = v$ and $mv^2/r \leqslant F$. Since both E and L are conserved, we need to satisfy the condition

$$\frac{L^2}{2mr^2} = \frac{1}{2}mv_\perp^2 \leqslant \frac{1}{2}mv^2 = E - Fr$$

at any point during the flyby. Rewriting we obtain

$$\frac{L^2}{2m} \leqslant Er^2 - Fr^3. \quad (3)$$

When $v_\perp = v$ we must have equality in Equation 3. Since all of the constants are positive the polynomial on the right

hand side has two roots at $r = 0$ and $r = E/F$ and one single maximum at $r = 2E/3F$. Therefore, there are two positive values $r_1 \leqslant r_2$ such that equality is attained, and for positive r the inequality is only satisfied in the interval $[r_1, r_2]$. This implies that circular capture can only occur at the two radii r_1 and r_2 and a flyby is only possible between these two boundaries. One of them is $r = r_i$ by construction as the initial $v_i = v_{i,\perp}$. Checking that

$$mv_i^2/r_i > F$$

ensures that the spacecraft is not immediately captured and hence $r_1 = r_i$ (instead of $r_2 = r_i$). Verifying that Equation 3 is satisfied at $r = r_f$ then ensures that for all intermediate $r_i < r < r_f$, and hence the entire flyby, no further circular capture can occur.

2.2. Deflection angle

Since we ensure that no circular capture can occur, the spacecraft is ensured to eventually reach the final radius r_f, where the tether is released. At that point, the energy is given by

$$E = \frac{1}{2}mv_f^2 + Fr_f$$

and hence solving for v_f we find

$$v_f = \sqrt{2m(E - Fr_f)}.$$

At the same time the angular momentum is given by

$$L = mv_{f,\perp}r_f$$

and hence

$$v_{f,\perp} = \frac{L}{mr_f} = \frac{v_i r_i}{r_f}.$$

The angle of the final velocity vector with respect to the radial direction is therefore given by

$$\beta = \arccos\left(\frac{v_{f,\perp}}{v_f}\right).$$

To compute the angle α of the radial direction between r_i and r_f, we use Binet's equation [6]:

$$\alpha = \frac{L}{\sqrt{2m}} \int_{1/r_f}^{1/r_i} \frac{u}{\sqrt{-Fu + Eu^2 - \frac{L^2 u^4}{2m}}} du. \quad (4)$$

Finally, the total deflection angle between the incoming and outgoing velocities in the local coordinate system is given by $\delta = \alpha - \beta$ (see Figure 1) and the energy difference is $\Delta E = F(r_f - r_i)$. This energy is either released as thermal energy due to friction, or can at least partly be converted into electrical energy by the tether unrolling mechanism on the spacecraft.

We remark that one can recover Equation 3 from Equation 4 by observing that the change in angle as a function of radius becomes singular (i.e. we enter circular motion) when the square root becomes zero which reduces exactly to the condition for no circular capture.

2.3. Solving the elliptic integral

The integral in Eq.(4) is an elliptic integral and can be solved in the most general case in terms of the Weierstrass elliptic and related functions: $\wp, \sigma, \zeta$ (see [7] for an extended introduction to these special functions). We rewrite the expression in the more convenient form:

$$\alpha = \frac{L}{\sqrt{2m}} \int_{1/r_f}^{1/r_i} \frac{u\,du}{\sqrt{au^4 + bu^2 + c}}$$

where $a = -\frac{L^2}{2m}$, $b = E$ and $c = -F$. In order to reduce the quartic polynomial to a cubic, we observe that zero is a root of the quartic polynomial and thus (see [8], Chapter 8) we may apply the substitution $u = \frac{1}{\xi}$ obtaining:

$$\alpha = \frac{L}{\sqrt{2m}} \int_{r_i}^{r_f} \frac{d\xi}{\xi\sqrt{c\xi^3 + b\xi^2 + a}}$$

We then bring the cubic in its depressed form (see [9], Appendix) using the substitution $\xi = \sqrt[3]{\frac{4}{c}}\eta - \frac{b}{3c}$ which results in a Weierstrass normal elliptic integral of the third kind:

$$\alpha = \frac{L}{\sqrt{2m}} \int_{\rho(r_i)}^{\rho(r_f)} \frac{d\eta}{\left(\sqrt[3]{\frac{4}{c}}\eta - \frac{b}{3c}\right)\sqrt{4\eta^3 - g_2\eta - g_3}}$$

where $\rho(\xi) = \sqrt[3]{\frac{c}{4}}\left(\xi + \frac{b}{3c}\right)$, $g_2 = \frac{b^2}{3c}\sqrt[3]{\frac{4}{c}}$, $g_3 = -\frac{2b^3}{27c^2} - a$. The final substitution $\eta = \wp(\omega)$ results in the expression:

$$\alpha = \frac{L}{\sqrt{2m}}\sqrt[3]{\frac{c}{4}} \int_{\tilde{\rho}(r_i)}^{\tilde{\rho}(r_f)} \frac{dw}{\wp(w) - \wp(\gamma)}$$

where $\tilde{\rho}(\xi) = \wp^{-1}(\rho(\xi))$ and $\wp(\gamma) = \frac{b}{3c}\sqrt[3]{\frac{c}{4}}$. We eventually obtain the final, analytical, expression:

$$\alpha = \frac{L}{\sqrt{2m}}\sqrt[3]{\frac{c}{4}}\left[\frac{1}{\wp'(\gamma)}\left(\log\frac{\sigma(w-\gamma)}{\sigma(w+\gamma)} + 2w\zeta(\gamma)\right)\right]_{\tilde{\rho}(r_i)}^{\tilde{\rho}(r_f)}$$

The evaluation of the Weierstrass elliptic and related functions appearing in the above integral can be efficiently made using modern computer implementations such as the open source one (C++ and python) available at:

`https://github.com/bluescarni/w_elliptic`
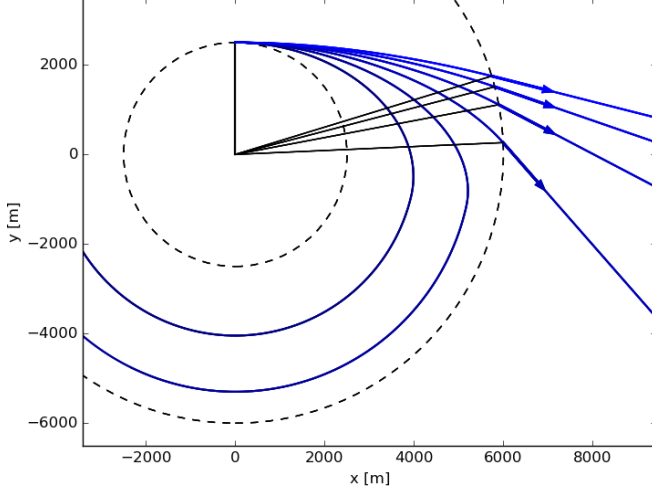
and described in [10].

Fig. 2. Example of a tethered flyby with different initial velocities v_i with analytically computed final velocity directions (arrows) as well as numerically computed trajectories (blue).
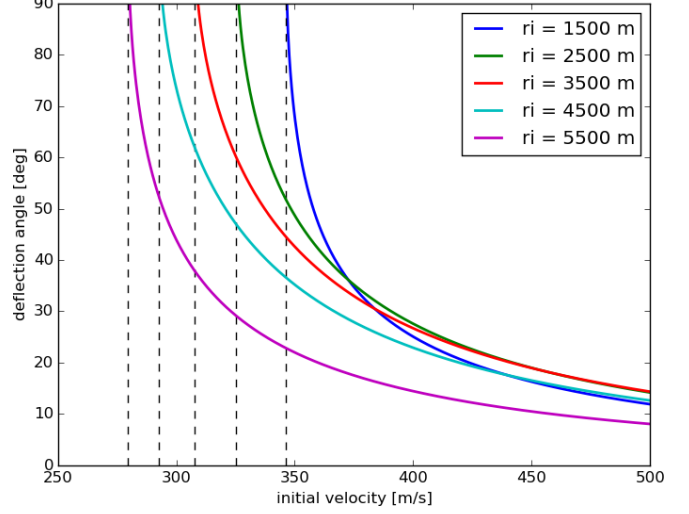

Fig. 3. Deflection angle achieved as a function of the initial velocity v_i and minimal required velocity to avoid circular capture (between $280 - 347$ m/s).

2.4. Tether tension

The total force at any point along the tether is caused by two effects: the force of the spacecraft on the tether given by F_r and an internal force due to the rotation of the massive tether itself [2]. In fact, the force at any point $\tilde{r}$ in a tether of uniform linear density μ and length r rotating around the origin with angular velocity ω is given by

$$F_t(\tilde{r}) = \int_{\tilde{r}}^{r} \mu r \omega^2 dr = \frac{1}{2}\mu \left(r^2 - \tilde{r}^2\right)\omega^2.$$

This force is maximal at the attachment point of the tether at $\tilde{r} = 0$ and since $\omega = v_i/r$ we have that

$$F_t = F_t(0) = \frac{1}{2}\mu r^2 \omega^2 = \frac{1}{2}\mu v_i^2.$$

Note that this expression only depends on the incoming velocity but is independent of the radial distance r of the closest approach.

The total maximum force in the tether is then $F_{max} = F_t + F_r$ and hence in order to limit the maximum force at any point in the tether to F_{max}, the parameter F in the force law F_r must be chosen as

$$F = F_{max} - F_t. \tag{5}$$

On the other hand, if a fixed F is to be used in Equation 1, then the maximum relative velocity for a flyby is limited by the condition $F_t \leqslant F_{max} - F$.

3. ANALYSIS

Figure 2 illustrates the orbits of various flybys at different initial velocities. The parameters for the flybys are

$$
\begin{aligned}
F &= 10 \text{ kN} \\
m &= 800 \text{ kg} \\
r_i &= 2500 \text{ m} \\
r_f &= 6000 \text{ m}
\end{aligned}
$$

and the initial velocities are chosen as

$$v_i \in [250, 300, 350, 400, 450, 500].$$

The initial velocities are shown in different shades of blue starting with dark blue for the lowest velocity. As can be seen, for $v_i = 250$ m/s and $v_i = 300$ m/s no flyby is possible because the spacecraft gets captured in a circular orbit before reaching the final radius. For the other velocities the spacecraft does reach the final radius and it is deflected to various degrees. As expected, the final deflection angle decreases monotonously with the initial velocity. The faster the spacecraft moves initially, the smaller the impact of the flyby maneuver is. This observation is confirmed in Figure 3, where the final deflection angle is shown as a function of initial velocity v_i for various initial radii r_i. Note that in all cases there is a minimum initial velocity required to achieve a full flyby, here between 280 m/s for $r_i = 550$ m and 347 m/s for $r_i = 1500$ m. Below this minimum v_i the spacecraft is captured in a circular orbit and does not complete the flyby. This is clear as for a sufficiently slow spacecraft capture would be immediate.

The same analysis can be made for the dependence on the initial flyby radius r_i. This is of particular interest as this pa-
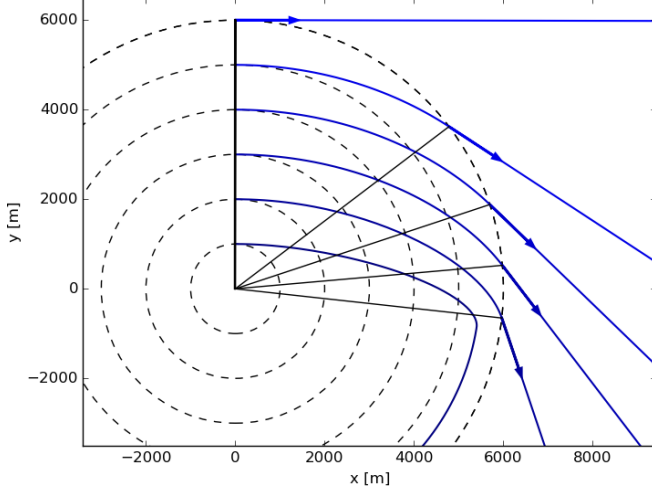
Fig. 4. Example of a tethered flyby with different initial radii r_i with analytically computed final velocity directions (arrows) as well as numerically computed trajectories (blue).
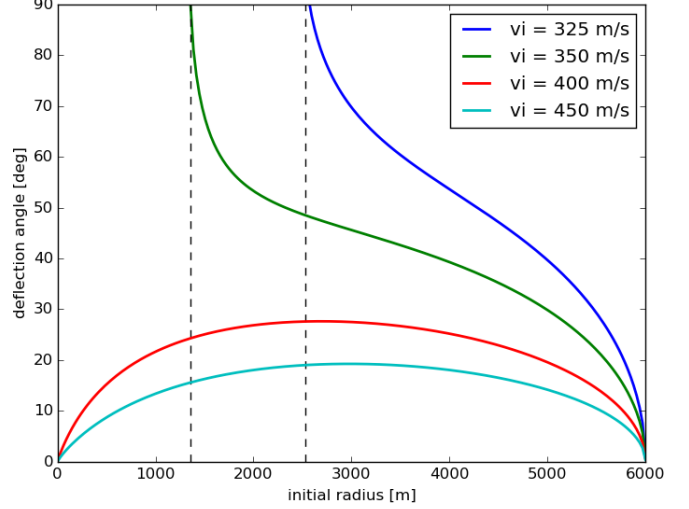

Fig. 5. Deflection angle achieved as a function of the initial radius r_i and minimal required radius to avoid circular capture where applicable (between $1357 - 2532$ m/s).

rameter is completely determined by the trajectory design and requires no changes to the mechanical setup of the spacecraft. As in the case of gravity assists, it is the free parameter than can be chosen by the trajectory designer to achieve the optimal deflection angle. Figure 4 shows several trajectories for $v_i = 340$ m/s and

$$r_i \in [1000, 2000, 3000, 4000, 5000, 6000].$$

m. All other parameters are kept as in the previous case. Setting the initial radius equal to the final radius obviously does not result in any change to the spacecraft velocity, which is clear. More interesting is the place where the maximum deflection is reached. For these values, it is towards the smallest allowable initial radius that does not lead to a captured orbit. However, this is not always the case. As can be seen in Figure 5, when the initial velocity is increased to a value such that no choice of initial radius leads to a captured orbit (i.e. all radii are allowed), the shape of the deflection curve changes completely. In this case, the deflection angle is zero for both $r_i = 0$ and $r_i = r_f$, while it has a maximum at roughly $(r_i + r_f)/2$.

Intuitively this behavior makes sense: for the hypothetical $r_i = 0$ case, there is no rotation and the only effect of the tether force is to slow down the spacecraft. If the initial energy (or equivalently the initial velocity) is sufficiently large, the spacecraft can still reach the final radius with only a change in final kinetic energy (and hence final velocity). This is not possible if the initial energy is too low and the spacecraft cannot reach r_f for energetic reasons. As r_i increases, the radial tether force starts to act in a direction different from the spacecraft velocity v, thus deflecting the orbit. However, as r_i approaches r_f, the time the spacecraft spends in the flyby reduces, effectively exposing the spacecraft to the de-

flecting force for a shorter time. In the limit $r_i = r_f$, the time spent in the flyby is 0 as the spacecraft immediately leaves the maximum tether radius, and hence no change in velocity occurs.

4. FLYBY SEQUENCING

To demonstrate how tethered flybys can be used in a mission design, we implemented a global search for a sequence of tethered asteroid flybys aided by chemical propulsion. More specifically, the spacecraft starts at some asteroid in the main asteroid belt and then use a sequence of other asteroids to tether to in order to reach the next asteroid in the sequence with the least amount of additional fuel used. The set of asteroids considered is an exhaustive database of 16256 main belt asteroids provided as part of the 7th edition of the Global Trajectory Optimization Contest (GTOC7) [11]. The asteroids are assumed to move on Keplerian orbits around the sun. The numeric IDs used to reference the asteroids in this paper are the same one-based indices used in the GTOC7 database. The asteroids of the main belt are particularly suitable for a tethered flyby mission because of their abundance and the fact that there are plenty of asteroids with relatively small differences in their orbits and hence relative velocities. This allows us to construct a sequence of asteroids with a required Δv at each asteroid on the order of hundreds of m/s. As the previous analysis has shown, this kind of Δv is feasible with tethered flybys.

The hypothetical spacecraft has an initial wet mass of 800 kg and is launched from a mothership that is in orbit with one of the asteroids. It receives an initial Δv of up to 1 km/s from the mothership in any direction. The launch date of the

emission is chosen between 11000 MJD and 12000 MJD (12 Feb 2030 - 8 Nov 2032). The maximum time for is fixed to a maximum of 6 years.

The tether is assumed to have a maximum safe force of $F_{max} = 10^4$ N and a maximum length of 6 km. Already with currently available materials, these specifications are feasible. Commercially available polyethylene fiber (such as Spectra 2000), for example, has a stress limit of 3 GPa and a density of 970 kg/m^3 [12]. A tether made from this material of a cross section of about 4 mm^2 hence has a linear density of about $\mu = 0.004$ kg/m yielding a total mass of less than 25 kg for the full length tether and a maximum safe force of $1.2 \cdot 10^4$ N. Using these values as a reference, we design each flyby not to exceed the maximum safe force F_{max} according to Equation 5. The only free parameter for each flyby is the initial flyby radius r_i. The minimum flyby radius is set to 1 km.

As the Δv produced by a single flyby is not always sufficient to produce the required change in orbit to reach the next asteroid in the sequence, we allow for one chemical burn per leg to provide additional Δv. The time of this burn can be anywhere along the leg, either as a boost right after the flyby or as a deep space maneuver in the middle of the leg.

4.1. Sequence optimization

For a given fixed sequence of asteroids, we have the following free variables to be determined:

1. starting epoch T_0,

2. angles u, v and magnitude V_{inf} of the initial Δv,

3. time of flight dt_i allocated for each leg,

4. fraction η_i of each leg's flight time at which a chemical burn is performed,

5. fraction ξ_i of the flyby radius at the beginning of each leg (except first leg),

6. angle β_i of the flyby plane at the beginning of each leg (except first leg).

In order to determine these values, we perform a global optimization using evolutionary optimization. To that end, we first implemented the above dynamics using PyKEP, a flexible and fast library of common astrodynamics routines with a convenient Python interface developed by the Advanced Concepts Team (ACT) at ESA [13]. The Python interface allows the quick and easy implementation and testing of new flyby dynamics such as the one presented in this work. We implement the dynamics as a function that given a flyby radius r_i and an orientation β returns the final velocity of the spacecraft after the flyby.

To optimize the open parameters of each leg, we use the open source optimization library PaGMO also developed at
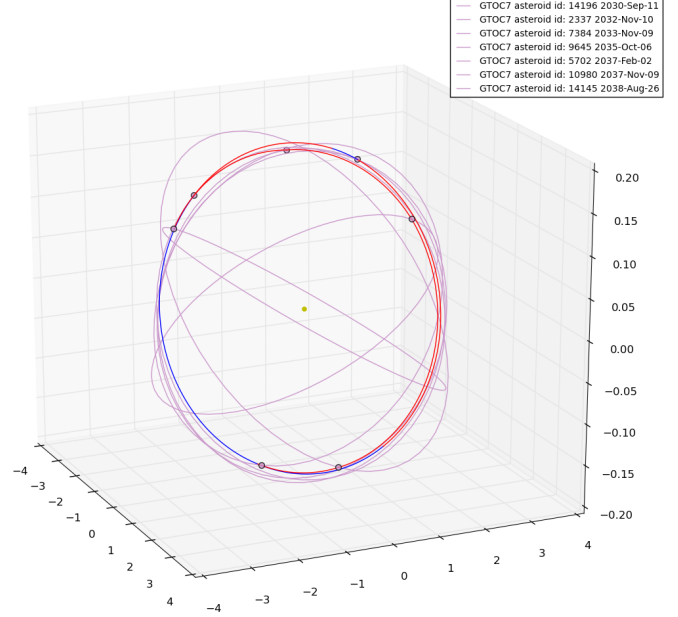

Fig. 6. Trajectory of a sequence of 7 asteroids connected by tethered flybys. Each leg before the deep space maneuver is shown in blue, afterwards in red.

the ACT [13]. Due to the open source nature of the tool, existing code for the optimization of classical gravity assist flyby sequences can easily be outfit with the new dynamics. The decision vector for the problem contains the free variables described above, with the limits given by the problem description. The cost function is the sum of all the impulsive Δv required to complete the sequence. It is assumed that the initial Δv is provided by the mothership and no attempt is made to match the orbit of the final asteroid in the sequence, so neither the initial V_{inf} nor the final excess velocity are taken into account.

4.2. Sequence generation

The sequence of asteroids to perform the flybys is generated incrementally. We start with three asteroids selected from previously computed GTOC7 solutions by the authors [14].

In order to extend the sequence by one more asteroid, we first filter the asteroid list using a KNN algorithm to compute the N nearest asteroids in a metric that takes into account both the orbit shape and the phasing relative to the last asteroid of the sequence and the arrival epoch. The rationale behind this approach is the observation that the relative velocity is crucial during a tethered flyby. Too high values for the relative velocity of asteroid and spacecraft cause the flyby to have virtually no effect. The best candidates for extending the sequence with minimal chemically provided Δv are typically found in the first 100 nearest asteroids.

To determine how much chemical fuel is needed to reach

Asteroid ID	Epoch [MJD2000]	r_i [m]	Flyby Δv [m/s]	Chemical Δv [m/s]
14196	11211.2	-	-	0.49
2337	12002.9	5891.8	27.6	0.22
7384	12366.6	3934.0	127.2	7.42
9645	13062.2	3957.6	33.6	42.6
5702	13547.9	3112.7	51.5	0.16
10980	13828.0	4910.7	133.6	0.26
14145	14117.4	-	-	-

Table 1. The identified sequence of 7 asteroids.

each possible next asteroid in the filtered set, we perform another optimization. First, we extract the final asteroid of the existing sequence, along with the arrival epoch t_f, and the velocity v_f at arrival of the spacecraft. Then a flyby is performed at radius r_f and orientation β_f, which is followed by a Lambert arc to reach the next asteroid candidate in time t. The cost of this flyby is estimated by considering the difference Δv_f in velocities after the flyby and the required initial velocity of the Lambert arc. An optimization is then carried out over r_f, β_f and t to minimize the mismatch Δv_f between the effect of the flyby and the velocity required to move to the next asteroid.

This optimization is notably simpler than the full sequence optimization described previously. While it does not yield the globally best solution even for this sequence, it is a fast and quite accurate measure of the quality of a candidate. In particular, if this local optimization finds a free transfer, this translates also into a free transfer for the optimal full sequence.

After selecting the most promising candidate asteroid, the sequence is extended and a full sequence optimization is performed before repeating the process.

We also tried to directly use GTOC7 sequences, but due to the different objectives of GTOC7 and this work the whole sequences do not yield good results for tethered flybys.

4.3. Result

We identified a sequence of 7 asteroids the can be connected by flybys. The total chemical Δv required for this mission is 51 m/s, while the flybys yield an additional Δv of 373 m/s. To complete the same trajectory using only chemical propulsion would require a Δv of about 235 m/s. We stopped at 7 asteroids but our experiments show that there is no limit at that value and that it is possible to build other and longer sequences as well.

Figure 6 shows the trajectories associated with the identified sequence. The asteroids visited, along with the epoch, flyby radius, and both the Δv resulting from the flyby as well as the Δv from the deep space maneuver are shown in Table 1.

It is interesting to note that the flyby radii are all above 3

km. The analysis in Section 3 suggests that the minimum for non-captured flybys occurs around that value, so this is understandable. The Δv amount in each flyby ranges from 27.6 m/s up to 133.6 m/s. The largest chemical deep space maneuver is required after the flyby of asteroid 9645, where over 80 % of the total chemical propulsion is needed. The other flybys are nearly completely passive with very little required chemical correction.

Another point worth mentioning is the location of the deep space maneuvers. While left free in the optimization problem formulation, the deep space maneuver most of the time occurs at the time of the flyby. This is due to the very similar orbits of the asteroids which do not benefit much from deep space corrections.

The initial Δv provided by the launcher and not included in this analysis is 0.5 km/s while the final excess velocity at asteroid 14145 is 1.44 km/s.

5. CONCLUSIONS

The dynamical model for tethered asteroid flybys with a force-limited tether developed in this paper lends itself to the global search for flyby sequencing. The analytical solution of the dynamics in terms of an elliptic integral or an elliptic function yields an efficient method for the calculation of the deflection of the spacecraft. The implementation of the dynamics in the PyKEP open source library for astrodynamics is straight forward due to the availability of the existing source code. The global optimization framework PaGMO allows the optimization of a flyby sequence of several asteroids in the asteroid belt.

To illustrate the effect of these flybys we constructed a sequence that requires significantly less Δv from chemical propulsion, 51 m/s, than a non-tethered alternative trajectory. The majority of the required total Δv comes from tethered flyby maneuvers contributing 373 m/s.

In this work we ignored the challenging the mechanical aspects of these tethered flybys such as attachment mechanisms and tether unwinding. However, our work shows that from a trajectory design perspective these types of flybys can provide significant Δv under realistic mission conditions. Also the tether requirements are within the realm of what can

be accomplished with today's tether materials. As such our proposed flybys are not as unrealistic as other advanced tether concepts which rely on hypothetical carbon nanotube tether materials.

6. REFERENCES

[1] A.V. Labunsky, O.V. Papkov, and K.G. Sukhanov, *Multiple Gravity Assist Interplanetary Trajectories*, Earth Space Institute Book Series. Taylor & Francis, 1998.

[2] Paul A. Penzo and Harris L. Mayer, "Tethers and asteroids for artificial gravity assist in the solar system," *J. Spacecraft and Rockets*, vol. 23, no. 1, pp. 79–82, January 1986.

[3] Eric L.-M. Lanoix and Arun K. Misra, "Near-earth asteroid and missions using and tether sling and shot assist," *Journal of spacecraft and rockets*, vol. 37, no. 4, pp. 475–480, July 2000.

[4] James R. Van Zandt, "Tethered asteroids," in *SPACE Conferences and Exposition*, pp. –. American Institute of Aeronautics and Astronautics, Sept. 2013.

[5] Antonio F. B. A. Prado, "Using tethered gravity-assisted maneuvers for planetary capture," *Journal of Guidance, Control, and Dynamics*, vol. 38, no. 9, pp. 1852–1856, September 2015.

[6] Herbert Goldstein, *Classical Mechanics*, Addison-Wesley, Reading, MA, 2nd edition edition, 1980.

[7] F. W. J. Olver, D. W. Lozier, R. F. Boisvert, and C. W. Clark, Eds., *NIST Handbook of Mathematical Functions*, Cambridge University Press, New York, NY, 2010, Print companion to [15].

[8] Zhu-Xi Wang, Dun Ren Guo, and XJ Xia, *Special functions*, vol. 15, World Scientific, 1989.

[9] Paul F Byrd and Morris David Friedman, *Handbook of elliptic integrals for engineers and scientists*, vol. 67, Springer Science & Business Media, 2012.

[10] Dario Izzo and Francesco Biscani, "On the astrodynamics applications of weierstrass elliptic and related functions," AAS 16-279. 26th AAS/AIAA Space Flight Mechanics Meeting, Napa, California, USA, February 2016.

[11] "Global trajectory optimization portal http://sophia.estec.esa.int/gtoc_portal/," .

[12] Jerome Pearson, Eugene Levin, John Oldson, and Harry Wykes, "Lunar space elevators for cislunar space development," Nasa final technical report, Star Technology and Research, Inc., 2005.

[13] Dario Izzo, "PyGMO and PyKEP: open source tools for massively parallel optimization in astrodynamics (the case of interplanetary trajectory optimization)," in *Proceedings of the Fifth International Conference on Astrodynamics Tools and Techniques, ICATT*, 2012.

[14] Mauro Massari and Alexander Wittig, "Optimization of multiple-rendezvous low-thrust missions on general-purpose graphics processing units," *Journal of Aerospace Information Systems*, pp. 1 – 13, Jan 2016.

[15] "NIST Digital Library of Mathematical Functions," http://dlmf.nist.gov/, Release 1.0.10 of 2015-08-07, Online companion to [7].